



A MODULE-BASED AND UNIFIED APPROACH TO CHAOTIC CIRCUIT DESIGN AND ITS APPLICATIONS

SIMIN YU

*College of Automation,
Guangdong University of Technology,
Guangzhou 510090, P. R. China*

JINHU LÜ*

*The Key Laboratory of Systems and Control, Institute of Systems Science,
Academy of Mathematics and Systems Science,
Chinese Academy of Sciences, Beijing 100080, P. R. China
Department of Ecology and Evolutionary Biology,
Princeton University, Princeton, NJ 08544, USA
jhlu@iss.ac.cn*

GUANRONG CHEN

*Department of Electronic Engineering,
City University of Hong Kong, Hong Kong SAR, P. R. China
gchen@ee.cityu.edu.hk*

Received December 15, 2005; Revised July 14, 2006

This paper proposes a module-based and unified approach to chaotic circuit design, where the description is based on the state equations without physical dimensions for simplicity of a general discussion. The main design process consists of transformation of state variables, transformation from differential to integral operations, and transformation of the time-scale. The designed circuit consists of anti-adder module integrator module, and inverter module. A novel 3-scroll Chua's circuit and a generalized Lorenz-like circuit are designed and implemented for verifying the effectiveness of this systematic circuit design methodology. Experimental observations are provided for confirmation. Comparing with the traditional circuit design methods, this new design approach has the following typical characteristics: (i) module-based and unified design; (ii) independent adjustment of system parameters; (iii) adjustment of distribution regions for the frequency spectra of chaotic signals; (iv) prominent observability.

Keywords: Chua's circuit; multi-scroll; module-based and unified circuit design; time-scale.

1. Introduction

Over the last four decades, chaos has been intensively investigated within the nonlinear science, information science, and engineering communities [Chen & Dong, 1998]. Aiming at real-world

applications, nonlinear circuit design has become a key issue in chaos-based technologies.

Remarkably, Chua's circuit [Chua *et al.*, 1986; Kennedy, 1993; Zhong *et al.*, 2002] is a paradigm in the nonlinear circuit theory. Based on Chua's

*Author for correspondence

circuit, many modified nonlinear circuits have been designed and implemented [Elwakil & Kennedy, 2000], including the MCK circuit [Matsumoto et al., 1986], revised Chua’s circuit [Yin, 1997], and various multi-scroll circuits [Han et al., 2005; Lü & Chen, 2006; Lü et al., 2004b; Lü et al., 2004c; Lü et al., 2006; Lü et al., 2003; Suykens & Vandewalle, 1993; Yalcin et al., 2000; Yalcin et al., 2002]. Most of these circuits are constructed by using capacitors, inductors and resistors along with Chua’s diode. In this paper, we propose a novel circuit design method in which the basic design idea is very different from Chua’s circuit but can realize the same chaotic dynamics and even much more.

As we know now, there are various design approaches of chaotic circuits by using various electronic or logic devices reported in the literature. For example, Elwakil et al. [2003] applied the so-called current feedback operational amplifiers (CFOAs) and digital logic operations to design the Lorenz-like circuit for implementing a four-wing butterfly attractor; Zhong and Tang [2002] designed the Chen circuit and Li et al. [2005] devised the hyperchaotic Chen circuit both based on the dimensionless state equations of the circuits. Most of the circuit design methods as above are not based on a common and unified framework and do not have the universality and compatibility. In the following, based on the dimensionless state equations of the circuit, a module-based and unified circuit design approach is then proposed. The designed circuit consists of three different functional blocks: anti-adder module, integrator module and inverter module. The main design process consists of transformation of state variables, transformation from differential to integral operations, and transformation of the time-scale. Comparing with the traditional circuit design methods, such as those of the Lorenz-like circuit [Elwakil et al., 2003], Chen circuit [Zhong & Tang, 2002], and hyperchaotic Chen circuit [Li et al., 2005], this new method has the following four typical characteristics: (i) module-based and unified design; (ii) independent adjustment of system parameters; (iii) adjustment of distribution regions for the frequency spectra of chaotic signals; (iv) prominent observability.

It should be especially pointed out that all state variables in the forms of the original or inverse variables input to the inverting terminals of the anti-adders and all noninverting terminals are connected to the earth in this proposed approach. However, in most traditional circuit design methods based

on the dimensionless state equations of the circuits [Zhong et al., 2002; Zhong & Tang, 2002; Li et al., 2005], all state variables simultaneously input to the inverting and noninverting terminals. Therefore, all parameters in our method are independently adjustable, however, all parameters in the traditional approaches as above are coupled together and not independently adjustable. To verify the effectiveness of this new approach, a novel 3-scroll Chua’s circuit and a generalized Lorenz-like circuit are designed and implemented with experimental observations provided for confirmation. Moreover, the proposed circuit design method can be easily and naturally generalized to the circuit designs of other chaotic circuits.

The rest of this paper is organized as follows. In Sec. 2, the new systematic circuit design approach is described and discussed. A novel 3-scroll Chua’s circuit and a generalized Lorenz-like circuit are then designed and implemented in Secs. 3 and 4, respectively, with experimental observations reported. Finally, some conclusions are drawn in Sec. 5.

2. A Module-Based and Unified Circuit Design Approach

This section proposes a module-based and unified circuit design approach, in which the fundamental design principle differs from those of the traditional circuit design methods.

This approach is based on the dimensionless state equations of the circuit. The main procedure can be summarized into three key steps; that is, Step I: *transformation of state variables*; Step II: *transformation from differential to integral operations*; Step III: *transformation of the time-scale*.

To start, consider a general system of n -dimensional state equations described by

$$\left\{ \begin{aligned} \frac{dx_1}{d\tau} &= \sum_{i=1}^n a_{1i}x_i + \sum_{j=1}^n \sum_{p=1}^n b_{jp}^1 x_j x_p \\ &\quad + \cdots + f_1(x_1, x_2, \dots, x_n) \\ \frac{dx_2}{d\tau} &= \sum_{i=1}^n a_{2i}x_i + \sum_{j=1}^n \sum_{p=1}^n b_{jp}^2 x_j x_p \\ &\quad + \cdots + f_2(x_1, x_2, \dots, x_n) \\ &\quad \dots \dots \dots \\ \frac{dx_n}{d\tau} &= \sum_{i=1}^n a_{ni}x_i + \sum_{j=1}^n \sum_{p=1}^n b_{jp}^n x_j x_p \\ &\quad + \cdots + f_n(x_1, x_2, \dots, x_n), \end{aligned} \right. \quad (1)$$

where the first sum represents the linear terms and the other sums are all cross products, with $f_i(x_1, x_2, \dots, x_n)$ ($1 \leq i \leq n$) being the different types of nonlinear functions, which can be saturated function series, hysteresis function series, step wave, sawtooth wave, triangular wave, transconductor wave and exponent functions, and so on.

It is well known that the dynamic regions of most electronic devices are very limited. For example, the linear dynamic region of the operational amplifier TL082 with electrical source of $\pm 15\text{ V}$ is only within $\pm 13.5\text{ V}$. However, for many chaotic systems, the dynamic regions of the state variables in the dimensionless state equations are far exceeding the linear dynamic regions of the operational amplifiers. To physically realize these chaotic systems, one has to compress the dynamic regions of all the state variables into the linear dynamic regions of the operational amplifiers. To do so, one may let $x'_i = kx_i$ ($1 \leq i \leq N$), where $k \leq 1$ is the compressed ratio. Then, according to Eq. (1), one has

$$\left\{ \begin{aligned} \frac{dx'_1}{d\tau} &= \sum_{i=1}^n a_{1i}x'_i + \frac{1}{k} \sum_{j=1}^n \sum_{p=1}^n b_{jp}^1 x'_j x'_p \\ &+ \dots + kf_1\left(\frac{x'_1}{k}, \frac{x'_2}{k}, \dots, \frac{x'_n}{k}\right) \\ \frac{dx'_2}{d\tau} &= \sum_{i=1}^n a_{2i}x'_i + \frac{1}{k} \sum_{j=1}^n \sum_{p=1}^n b_{jp}^2 x'_j x'_p \\ &+ \dots + kf_2\left(\frac{x'_1}{k}, \frac{x'_2}{k}, \dots, \frac{x'_n}{k}\right) \\ &\dots\dots\dots \\ \frac{dx'_n}{d\tau} &= \sum_{i=1}^n a_{ni}x'_i + \frac{1}{k} \sum_{j=1}^n \sum_{p=1}^n b_{jp}^n x'_j x'_p \\ &+ \dots + kf_n\left(\frac{x'_1}{k}, \frac{x'_2}{k}, \dots, \frac{x'_n}{k}\right). \end{aligned} \right. \quad (2)$$

It is quite easy to obtain the integral form of Eq. (2), based on which one can further get the final circuit equation by using a transformation of the time-scale. According to the above circuit equation, one can easily design a block circuit diagram, which includes three main modules: *anti-adders module* *integrators module* and *inverters module*.

In the following, this circuit design approach is illustrated by working out two typical examples: a novel 3-scroll Chua's circuit and a generalized Lorenz-like system.

3. A Novel 3-Scroll Chua's Circuit

It is known that the piecewise linear function in the original Chua's circuit can be replaced by other nonlinear functions, such as the sine function [Tang *et al.*, 2001], exponent function [Abdomerovic *et al.*, 2000], and polynomial function [Tang & Man, 1998; Zhong, 1994], so as to generate various double-scroll or even multi-scroll chaotic attractors from the circuit [Yu *et al.*, 2004a; Yu *et al.*, 2004b; Yu *et al.*, 2005]. Here, we are especially interested in polynomial characteristic functions, such as $ax+bx|x|$, $ax+bx^3$, $a+bx+cx^2+dx^3$, etc. Notice that all these polynomial characteristic functions can only generate double-scroll Chua's attractors. To create more scrolls in Chua's circuit, the polynomial characteristic function is first modified to be $ax+bx|x|+cx^3$. Thus, Chua's circuit equation becomes

$$\begin{cases} \frac{dx}{d\tau} = \alpha(y - h(x)) \\ \frac{dy}{d\tau} = x - y + z \\ \frac{dz}{d\tau} = -\beta y, \end{cases} \quad (3)$$

where $\alpha = 12.8, \beta = 19.1, h(x) = ax + bx|x| + cx^3$. When $a = 0.472, b = -1, c = 0.47$, the polynomial characteristic curve is shown in Fig. 1. Here, five equilibria, four turning points and five characteristic regions are denoted by x_i ($0 \leq i \leq 4$), e_i ($1 \leq i \leq 4$) and D_i ($0 \leq i \leq 4$), respectively. Figure 2 shows the numerical simulation results of the

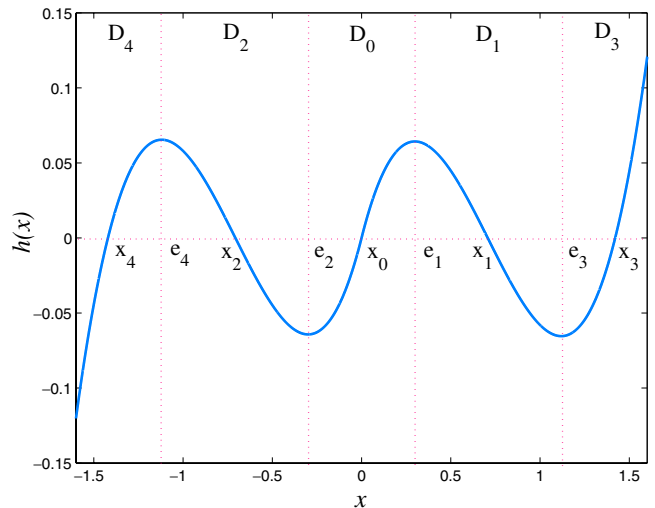


Fig. 1. $h(x)$ and its five characteristic regions.

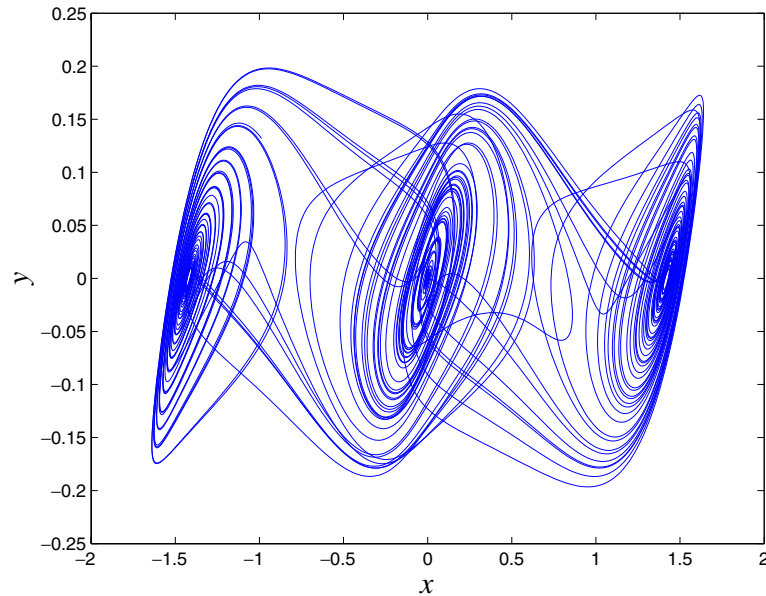
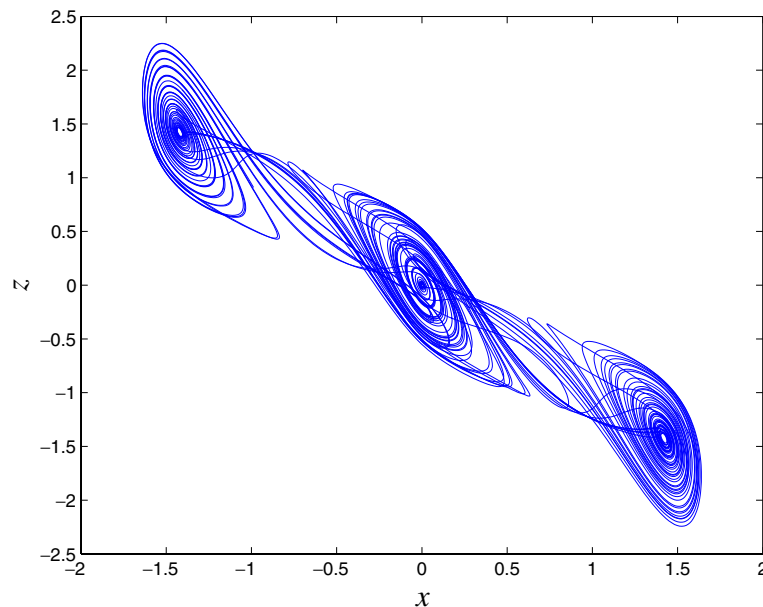
(a) $x - y$ plane(b) $x - z$ plane

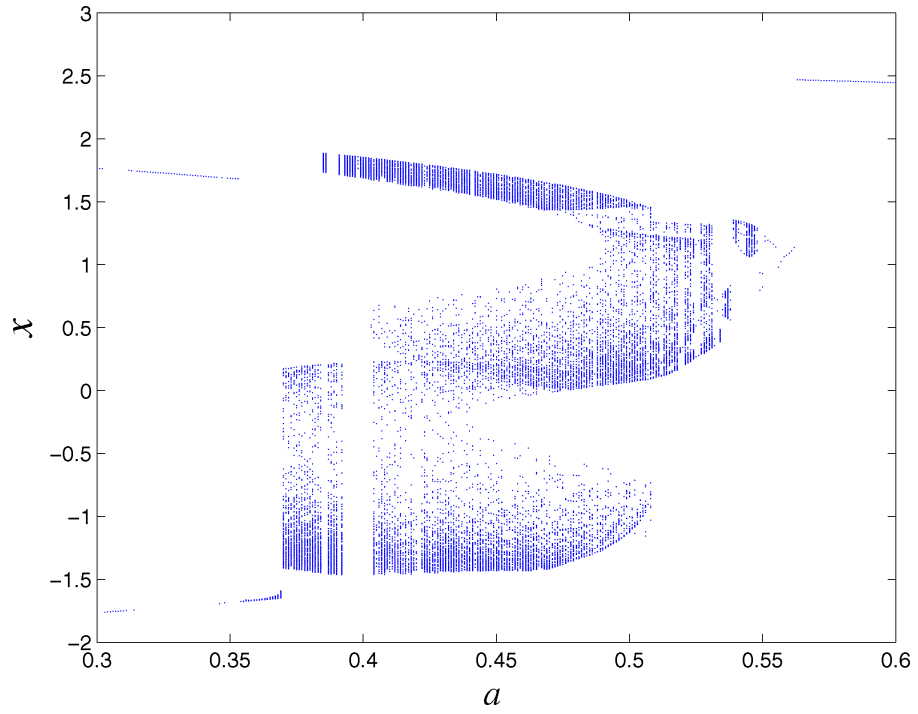
Fig. 2. Plane projection of the 3-scroll Chua's attractor.

3-scroll Chua's attractor with Lyapunov exponents: $\lambda_1 = 0.2$, $\lambda_2 = 0$, $\lambda_3 = -5.56$.

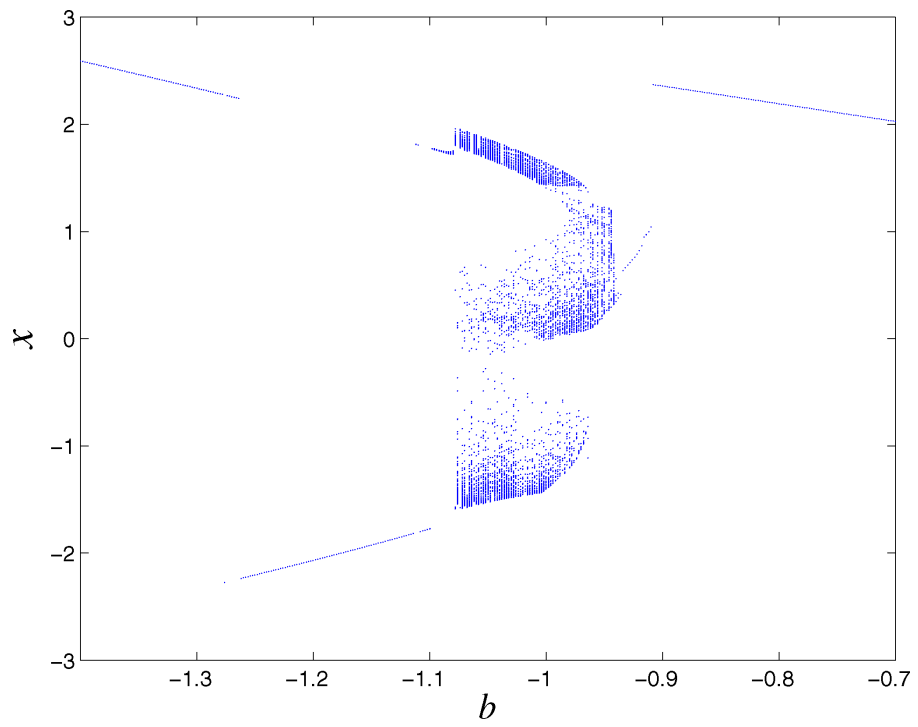
Both theoretical analysis and numerical simulations show that there are various bifurcation phenomena in system (3). Figures 3(a)–3(d) show the bifurcation diagrams versus parameter a with $\alpha = 12.8$, $\beta = 19.1$, $b = -1$, $c = 0.47$, parameter b with $\alpha = 12.8$, $\beta = 19.1$, $a = 0.472$, $c = 0.47$,

parameter c with $\alpha = 12.8$, $\beta = 19.1$, $a = 0.472$, $b = -1$, and parameter α with $\beta = 19.1$, $a = 0.472$, $b = -1$, $c = 0.47$, respectively. According to Fig. 3, there are some continuous chaotic regions for parameters α, a, b, c , which are very useful for hardware implementation.

When $a = 0.472$, $b = -1$, $c = 0.47$, system (3) has five equilibria: $(x_i, 0, -x_i)$ ($0 \leq i \leq 4$), where

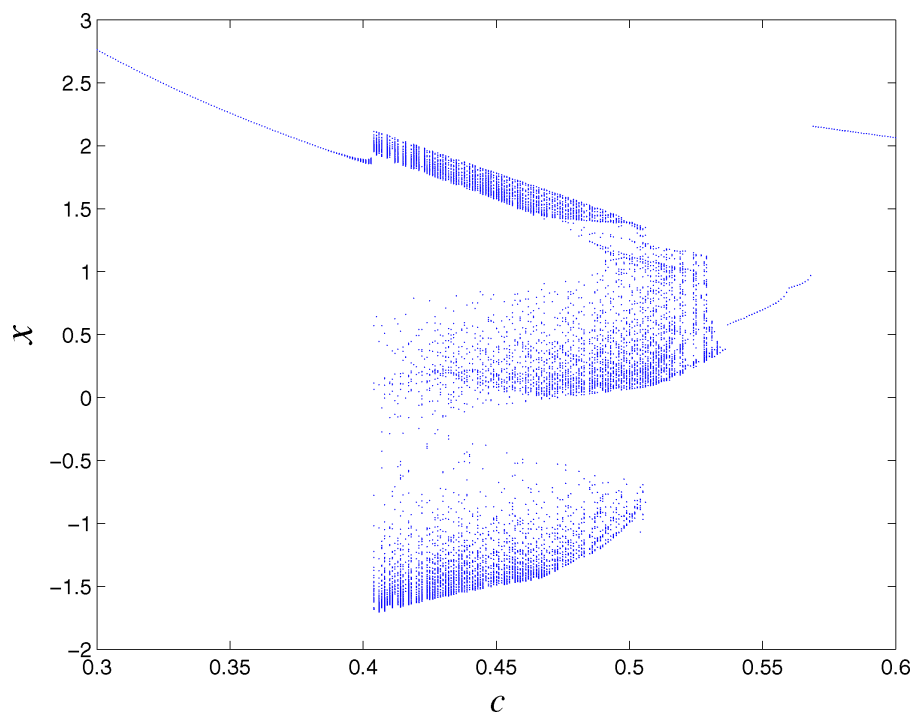


(a)

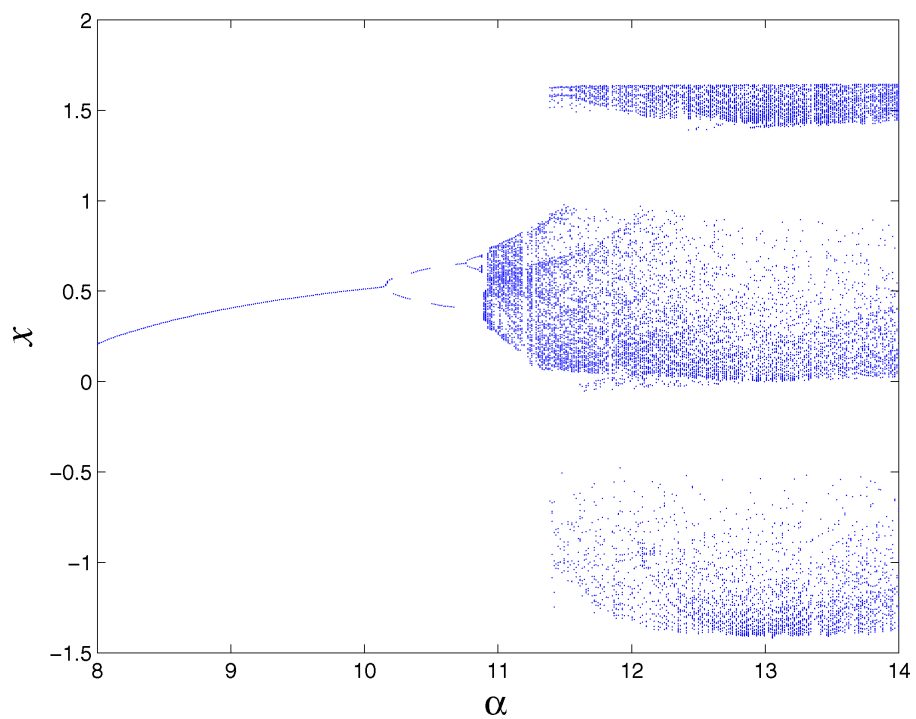


(b)

Fig. 3. Bifurcation diagrams of parameters a, b, c, α .



(c)



(d)

Fig. 3. (Continued)

$x_0 = 0, x_{1,2} = \pm 0.7068, x_{3,4} = \pm 1.4209$. Moreover, the Jacobians of system (3) evaluated at its equilibria $(x_i, 0, -x_i) (0 \leq i \leq 4)$ are given by

$$J(x_i) = \begin{pmatrix} -\alpha \frac{dh(x)}{dx} \Big|_{x=x_i} & \alpha & 0 \\ 1 & -1 & 1 \\ 0 & -\beta & 0 \end{pmatrix}$$

for $0 \leq i \leq 4$. Their corresponding eigenvalues are: $\gamma_0 = -7.4606, \sigma_0 \pm j\omega_0 = 0.2095 \pm j3.9273, \gamma_{1,2} = 4.3504, \sigma_{1,2} \pm j\omega_{1,2} = -1.1570 \pm j3.4629$, and $\gamma_{3,4} = -7.5171, \sigma_{3,4} \pm j\omega_{3,4} = 0.2066 \pm j3.9328$, respectively. Obviously, x_0, x_3, x_4 are the equilibria with index 2, which can generate scrolls in the attractor; on the other hand, x_1, x_2 are the equilibria with index 1, which can connect neighboring scrolls in the attractor.

In the following, a circuit diagram is designed to physically realize the above 3-scroll Chua's attractor. According to the circuit design method introduced in Sec. 2, one firstly gets the corresponding Eq. (3) after transformation of state variables, as follows:

$$\begin{cases} \frac{du}{d\tau} = \alpha \left[v - \left(au + \frac{b}{k}u|u| + \frac{c}{k^2}u^3 \right) \right] \\ \frac{dv}{d\tau} = u - v + w \\ \frac{dw}{d\tau} = -\beta v, \end{cases} \quad (4)$$

where k is the compressed ratio. From Fig. 2, one can see that the dynamic regions of all the state variables of system (3) belong to the linear dynamic regions of the operational amplifiers. In this case, one may simply let $k = 1$.

Thus, the integral form of system (4) is given by

$$\begin{cases} u = \int [-a_{11}(-v) - a_{12}h(u)]d\tau \\ v = \int [-a_{21}(-u) - a_{22}v - a_{23}(-w)]d\tau \\ w = \int -a_{31}vd\tau, \end{cases} \quad (5)$$

where $a_{ij} (1 \leq i, j \leq 3)$ are system parameters and $a_{11} = a_{12} = \alpha = 12.8, a_{13} = a_{32} = a_{33} = 0, a_{21} = a_{22} = a_{23} = 1, a_{31} = \beta = 19.1. h(u) = au + (b/k)u|u| + (c/k^2)u^3, a = 0.472, b = -1, c = 0.47, k = 1$. Based on system (5), one

can design a block circuit diagram to physically realize the 3-scroll Chua's attractor, as shown in Fig. 4.

All operational amplifiers shown in Fig. 4 are TL082, the supply voltages of the positive and negative electrical sources are $\pm 15V$. Moreover, for convenient adjustment and higher precision, all resistors are precisely adjustable resistors or potentiometers. In addition, in Fig. 4, the operational amplifiers OP1, OP4, OP7 are anti-adder modules; the operational amplifiers OP2, OP5, OP8 are anti-integrator modules; the operational amplifiers OP3, OP6, OP9 are inverter modules. Figures 4(a) and 4(b) are the basic Chua's circuit and polynomial signal generator for $h(u) = au + (b/k)u|u| + (c/k^2)u^3$, respectively. Here, the absolute-value circuit is shown in the dashed-line block of Fig. 4(b). From the generalized superposition principle, the relationship between input and output of the absolute-value circuit satisfies $u_0 = -u - 2u_1$. For $u < 0$, the diodes D_1 and D_2 are connected and $u_1 = 0$. Thus, $u_0 = -u > 0$. For $u > 0$, the diodes D_1 and D_2 are disconnected and $u_1 = -u$. Thus, $u_0 = -u + 2u = u > 0$. Therefore, $u_0 = |u|$.

According to Fig. 4(b), the relationship between the input and the output of the polynomial signal generator is described by

$$h(u) = \frac{R_n}{R_a}u - \frac{R_n}{10R_b}u|u| + \frac{R_n}{100R_c}u^3 \quad (6)$$

where $a = R_n/R_a, b/k = -(R_n/10R_b), c/k^2 = R_n/100R_c, k = 1$. When R_n is fixed, one can adjust the system parameters $a, b/k, c/k^2$ of polynomial $h(u)$ by adjusting the resistors R_a, R_b, R_c , respectively.

It follows from Fig. 4(a) that the state equation of the nonlinear circuit is given by

$$\begin{cases} u = \frac{1}{R_0C_0} \int \left[-\frac{R_f}{R_{11}}(-v) - \frac{R_f}{R_{12}}h(u) \right] dt \\ v = \frac{1}{R_0C_0} \int \left[-\frac{R_f}{R_{21}}(-u) - \frac{R_f}{R_{22}}v - \frac{R_f}{R_{23}}(-w) \right] dt \\ w = \frac{1}{R_0C_0} \int \left[-\frac{R_f}{R_{31}}v \right] dt. \end{cases} \quad (7)$$

Let $\tau = t/R_0C_0$. Here, $1/R_0C_0$ is the integral constant of the integrators shown in Fig. 4(a), which is also the transformation factor of the time-scale.

Then, one obtains

$$\begin{cases} u = \int \left[-\frac{R_f}{R_{11}}(-v) - \frac{R_f}{R_{12}}h(u) \right] d\tau \\ v = \int \left[-\frac{R_f}{R_{21}}(-u) - \frac{R_f}{R_{22}}v - \frac{R_f}{R_{23}}(-w) \right] d\tau \\ w = \int \left[-\frac{R_f}{R_{31}}v \right] d\tau. \end{cases} \quad (8)$$

According to (5) and (8), all system parameters are given by $a_{11} = R_f/R_{11}$, $a_{12} = R_f/R_{12}$, $a_{21} = R_f/R_{21}$, $a_{22} = R_f/R_{22}$, $a_{23} = R_f/R_{23}$, $a_{31} = R_f/R_{31}$. Let $R_f = 100k$, $R_{11} = 7.8k$, $R_{12} = 7.8k$, $R_{21} = 100k$, $R_{22} = 100k$, $R_{23} = 100k$, $R_{31} = 5.3k$. Then, one has $a_{11} = a_{12} = 12.8$, $a_{21} = a_{22} = a_{23} = 1$, $a_{31} = 19.1$. Since there are three anti-adder modules in Fig. 4, for a fixed

R_f , one can independently adjust various system parameters, $a_{ij}(1 \leq i, j \leq 3)$, by tuning the corresponding resistors $R_{ij}(1 \leq i, j \leq 3)$ in Fig. 4, respectively. Therefore, this independently adjustable characteristic is one of the useful features of the modular circuit design. Figure 5 shows the experimental observations of the 3-scroll Chua's attractor.

From (7), the transformation factor of the time-scale is completely determined by the integral resistor R_0 and integral capacitance C_0 . Comparing with the traditional design methods, such as that of Chua's circuit, this module-based and unified design approach can change the distribution region of the frequency spectrum of a chaotic signal as required by tuning integral resistor R_0 or integral capacitance C_0 for real-world applications. That is, when R_0 (or C_0) is decreasing, one can

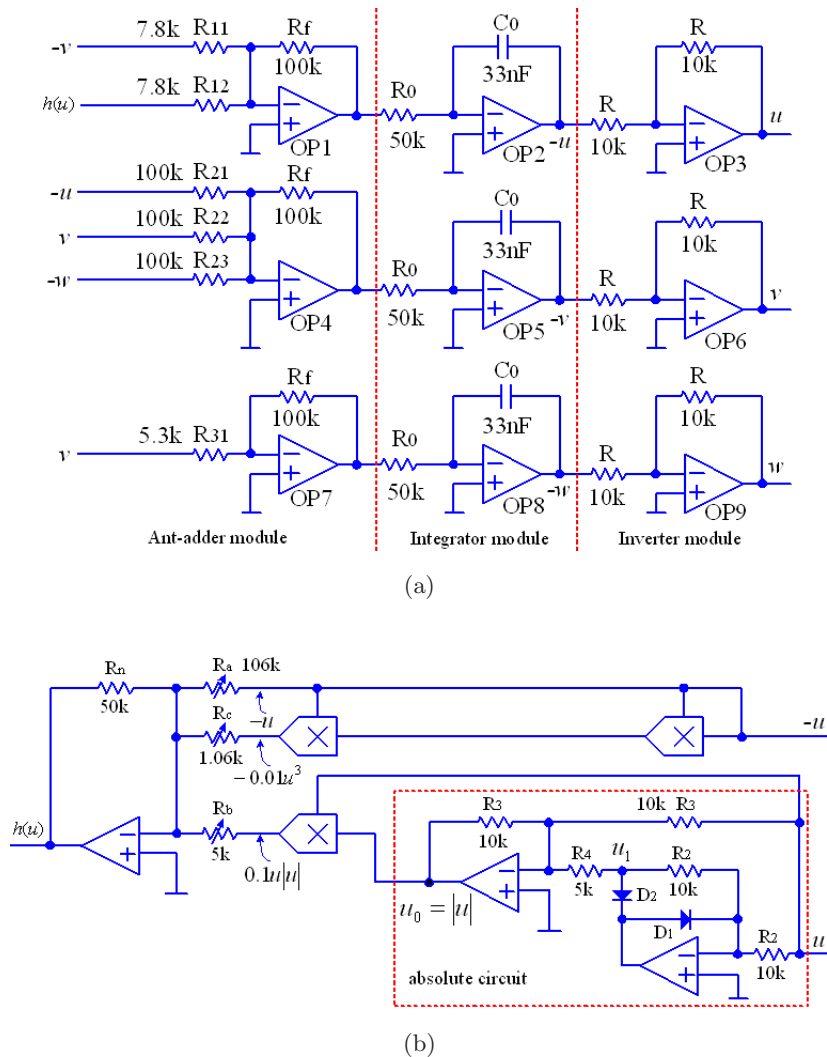
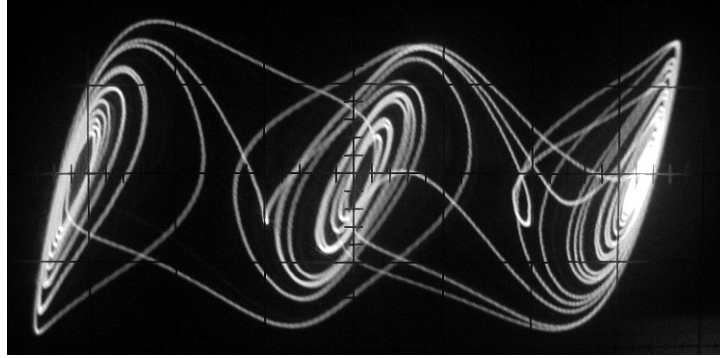
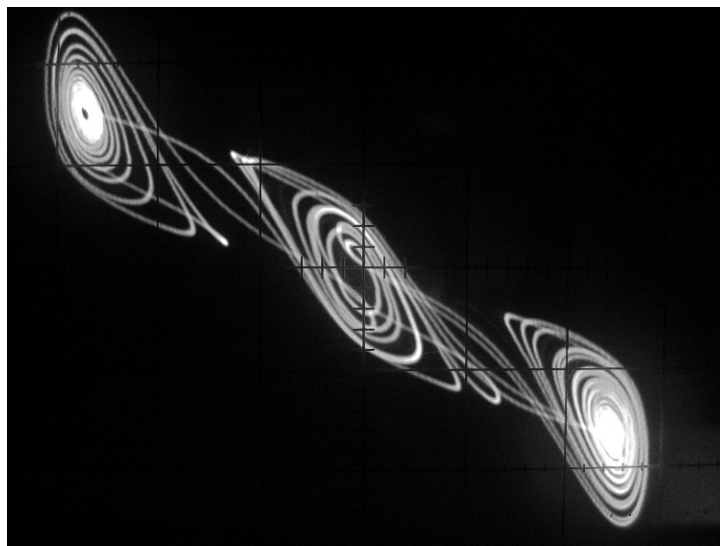


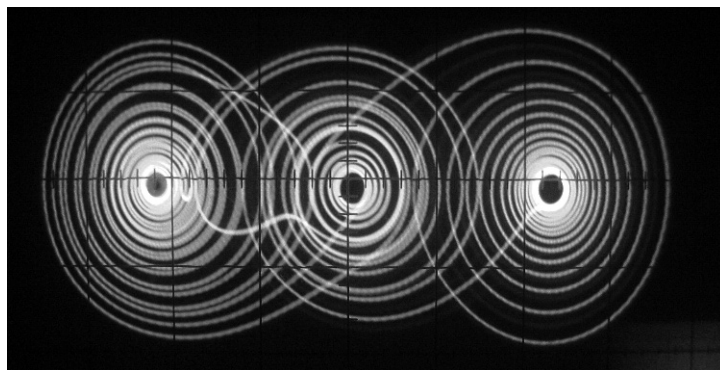
Fig. 4. Circuit diagram for realizing the 3-scroll Chua's attractor.



(a) $x - y$ plane, where $x = 0.5 \text{ V/div}$, $y = 1.0 \text{ V/div}$



(b) $x - z$ plane, where $x = 1 \text{ V/div}$, $z = 0.6 \text{ V/div}$

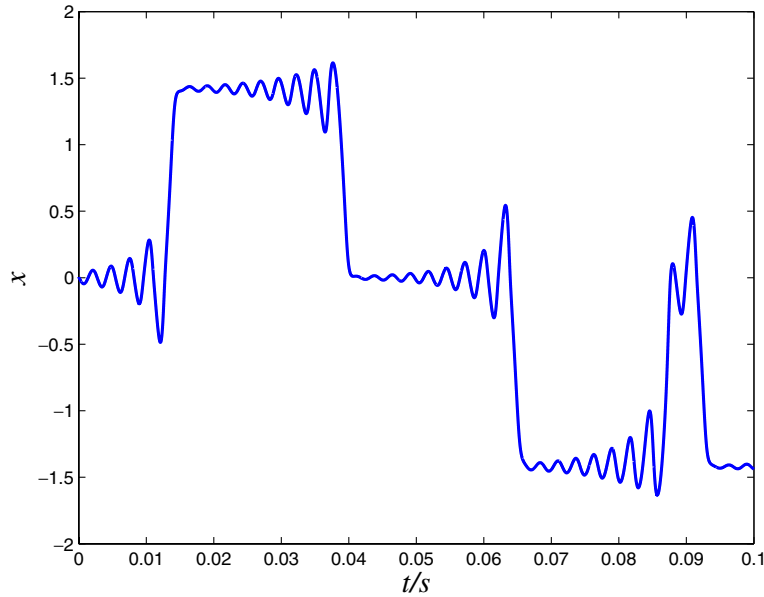


(c) $y - z$ plane, where $y = 1 \text{ V/div}$, $z = 0.6 \text{ V/div}$

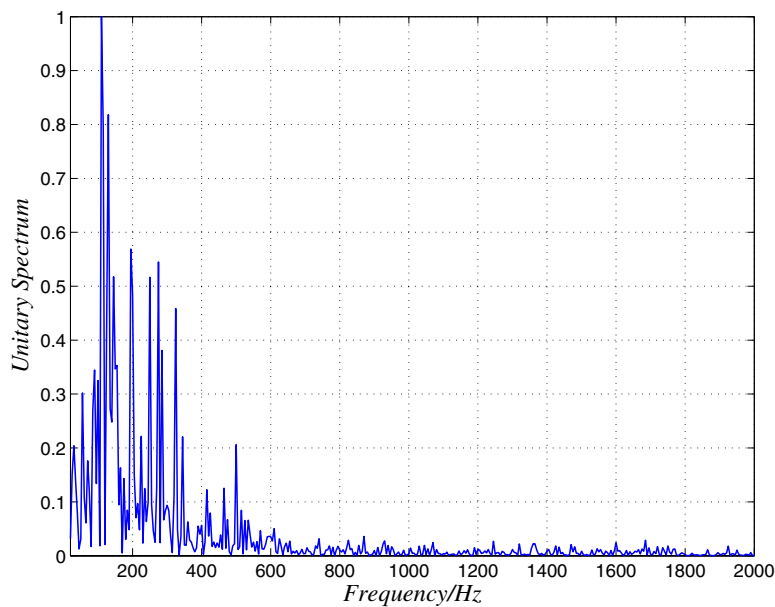
Fig. 5. Experimental observations of the 3-scroll Chua's attractor.

extend the distribution region of the frequency spectrum of the high-frequency end of a chaotic signal. However, when R_0 (or C_0) is increasing, one can reduce the distribution region of the frequency spectrum of the high-frequency end of a chaotic signal. Therefore, comparing with the fixed capacitance and inductance in Chua's circuit, this adjusting characteristic is very useful for real circuit design and practical engineering applications.

Here, two typical examples are used to show the effectiveness of this proposed design method. Figure 6 shows the waveforms and power spectrums of the time domain of the variable x for two different cases: (I) $C_0 = 33\text{ nF}$, $R_0 = 50\text{ k}\Omega$ and (II) $C_0 = 33\text{ nF}$, $R_0 = 10\text{ k}\Omega$, respectively, where the other parameters are given in Fig. 4. Our experimental observations are consistent with the numerical observations in Fig. 6.

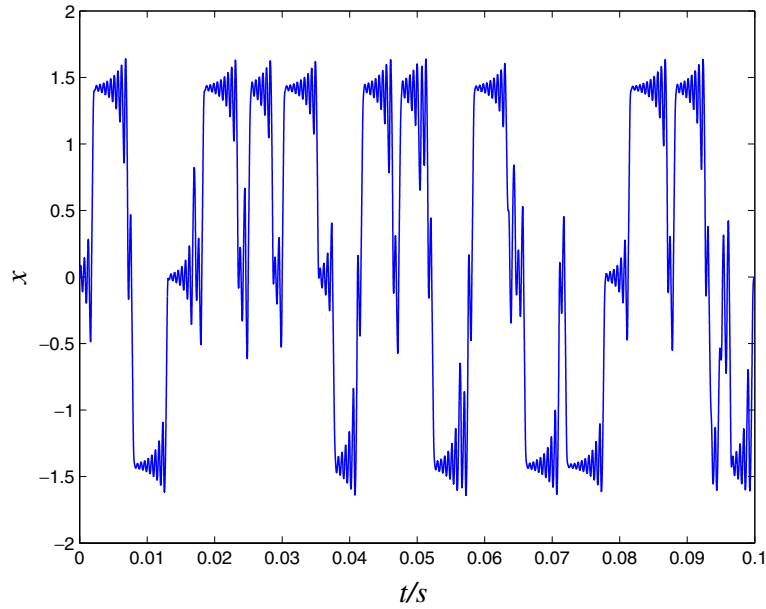


(a) Waveform of x , $C_0 = 33\text{ nF}$, $R_0 = 50\text{ k}\Omega$

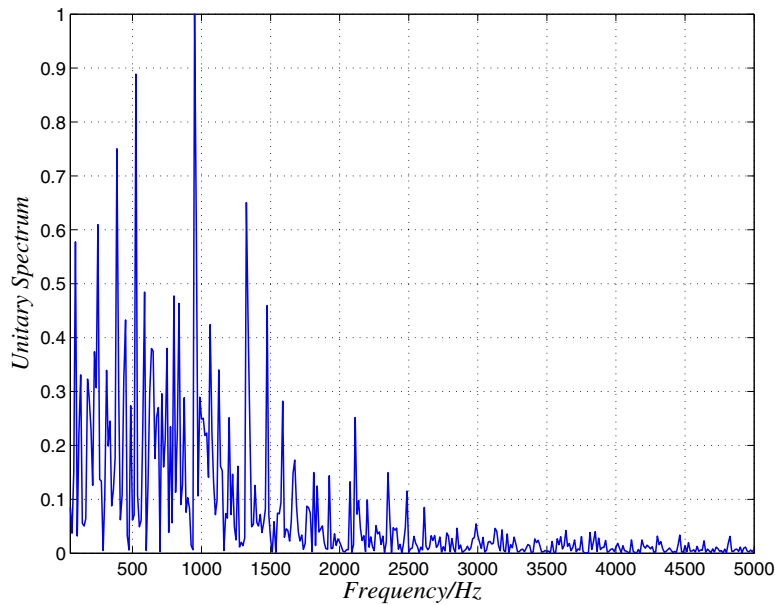


(b) Power spectrum of x , $C_0 = 33\text{ nF}$, $R_0 = 50\text{ k}\Omega$

Fig. 6. Numerical simulations of the waveforms and power spectrums of variable x .



(c) Waveform of x , $C_0 = 33 \text{ nF}$, $R_0 = 10 \text{ k}\Omega$



(d) Power spectrum of x , $C_0 = 33 \text{ nF}$, $R_0 = 10 \text{ k}\Omega$

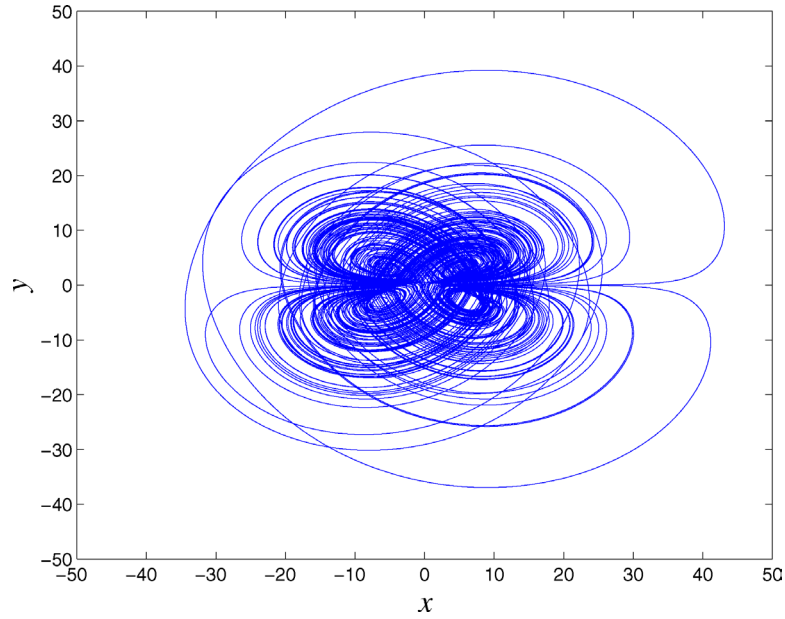
Fig. 6. (Continued)

It is well known that almost all design methods of chaotic circuit are not beautiful. Comparing with the traditional design approaches, such as that of Chua's circuit, the main disadvantage of the proposed design method is that it is likely to need more electronic devices. More electronic devices may increase the total hardware errors. However, one can minimize the total hardware

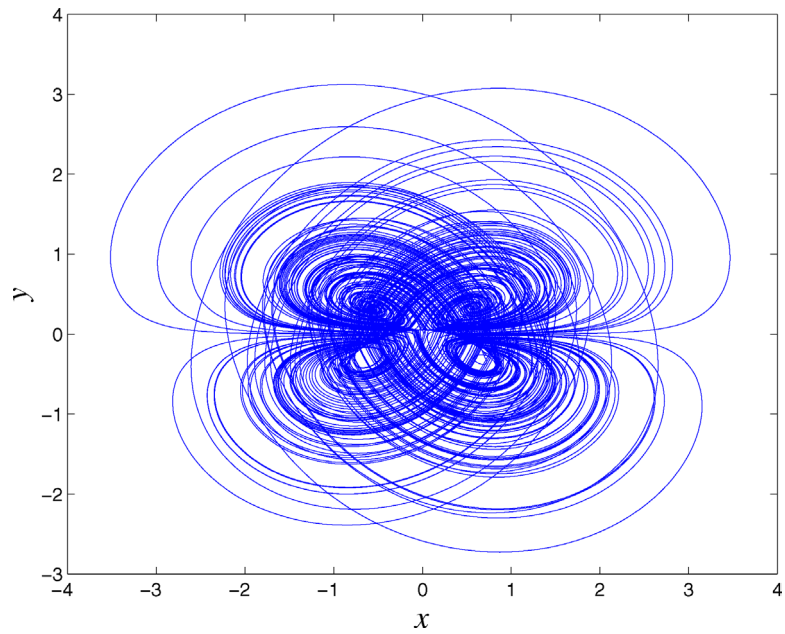
errors by using the electronic devices with high precision.

4. Circuit Implementation of a Generalized Lorenz-like System

A generalized Lorenz-like system was proposed in [Lü & Chen, 2002; Lü *et al.*, 2002], which is



(a) Original attractor



(b) Compressed attractor

Fig. 7. Numerical simulations of the generalized Lorenz-like system.

described by

$$\begin{cases} \frac{dx}{d\tau} = \frac{ab}{a+b}x - yz \\ \frac{dy}{d\tau} = -ay + xz + d \\ \frac{dz}{d\tau} = -bz + xy. \end{cases} \quad (9)$$

When $a = 10, b = 5, d = 5$, system (9) has a Lorenz-like chaotic attractor [Lü et al., 2004a], as shown in Fig. 7(a).

Obviously, the dynamic regions of the state variables x, y, z of system (8) are far exceeding the linearly dynamic regions of the operational amplifiers. To physically realize system (9), one has to compress the dynamic regions of the state variables x, y, z . To do so, let $u = kx, v = ky, w = kz$, where

$k = 0.1$. Then, one gets

$$\begin{cases} \frac{du}{d\tau} = \frac{ab}{a+b}u - vw \\ \frac{dv}{d\tau} = -av + 10uw + 10d \\ \frac{dw}{d\tau} = -bw + 10uv. \end{cases} \quad (10)$$

When $a = 10, b = 5, d = 5$, system (10) has a chaotic attractor as shown in Fig. 7(b). Obviously,

the dynamic regions of the state variables x, y, z of system (10) are compressed to be within the linear dynamic regions of the operational amplifiers.

Similarly, based on the circuit design principle proposed in Sec. 2, one can construct a circuit diagram, as shown in Fig. 8, to physically realize system (10). Figure 9 shows the experimental observations of the 4-scroll generalized Lorenz-like chaotic attractor.

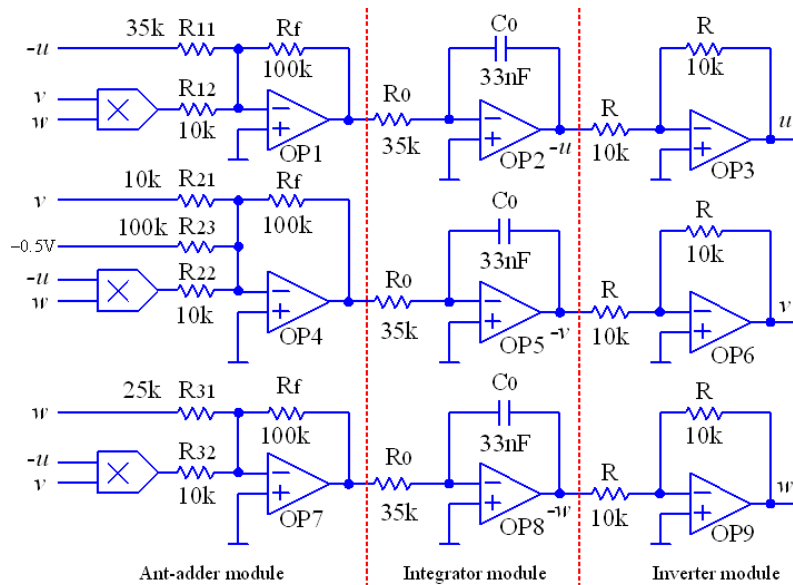
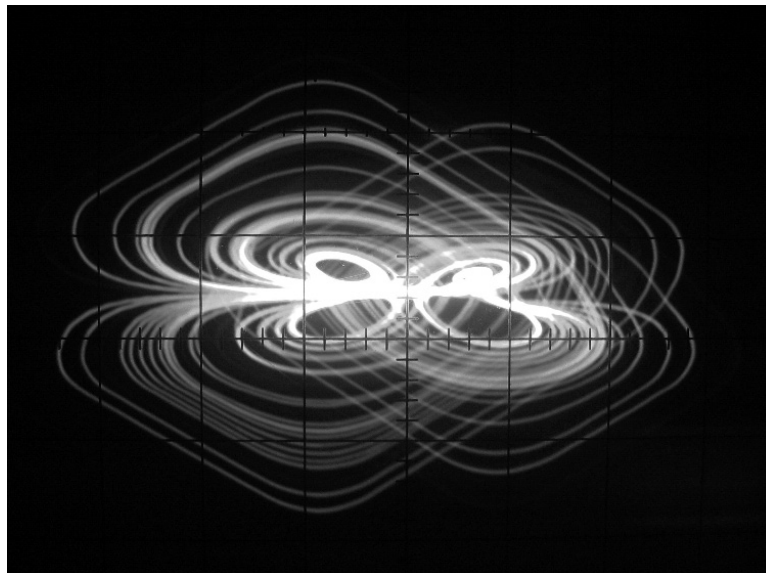
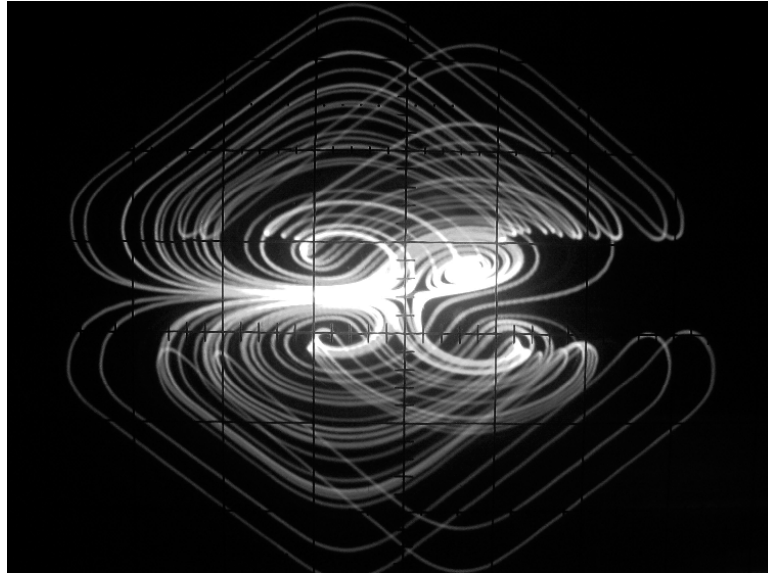
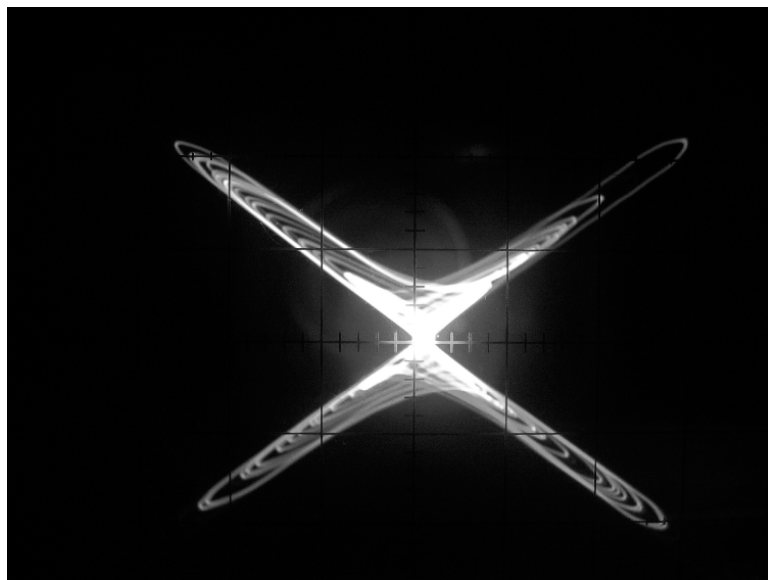


Fig. 8. Circuit diagram for realizing the generalized Lorenz-like system.



(a) $x - y$ plane, $x = 1.0 \text{ V/div}$, $y = 0.6 \text{ V/div}$

Fig. 9. Experimental observations of the generalized Lorenz-like system.

(b) $x - z$ plane, $x = 1.0 \text{ V/div}$, $z = 1.0 \text{ V/div}$ (c) $y - z$ plane, where $y = 1.0 \text{ V/div}$, $z = 1.2 \text{ V/div}$ Fig. 9. (*Continued*)

5. Conclusions

We have introduced a module-based and unified approach to chaotic circuit design. This method is based on the dimensionless state equations, and the main design process consists of transformation of state variables (which extends the parameter ranges in hardware implementation of nonlinear circuits), transformation from differential to integral operations, and transformation of the time-scale. The designed circuit includes

three different function blocks: anti-adder module integrator module and inverter module. Comparing with the traditional circuit design methods, this systematic approach has the following four typical characteristics: (i) module-based and unified design; (ii) independent adjustment of system parameters; (iii) adjustment of distribution regions for the frequency spectra of chaotic signals; (iv) prominent observability. To measure the current of the inductance of Chua's circuit, an additional circuit is needed to perform the

current-voltage transformation. Moreover, a novel 3-scroll Chua's circuit and a generalized Lorenz-like circuit have been designed and implemented to verify the effectiveness of the new design methodology, furthermore confirmed by experimental observations. It is believed that this module-based and unified circuit design approach will have good applications in practice.

Acknowledgments

This work was supported by the National Natural Science Foundation of China under Grants No. 60304017, No. 6022130, No. 20336040 and No. 60572073, the Scientific Research Startup Special Foundation on Excellent PhD thesis and the Presidential Award of Chinese Academy of Sciences, Natural Science Foundation of Guangdong Province under Grants No. 32469 and No. 5001818, Science and Technology Program of Guangzhou City under Grant No. 2004J1-C0291, Important Direction Project of Knowledge Innovation Program of Chinese Academy of Sciences under Grant KJCX3-SYW-S01, and the City University of Hong Kong under the SRG grant 7002134.

References

- Abdomerovic, I., Lozowski, A. G. & Aronhime, P. B. [2000] "High-frequency Chua's circuit," *Proc. 43th IEEE Midwest Symp. Circuits and Systems*, Lansing MI, USA, Aug. 8–11, pp. 1026–1028.
- Chen, G. & Dong, X. [1998] *From Chaos to Order: Methodologies, Perspectives and Applications* (World Scientific, Singapore).
- Chua, L. O., Komuro, M. & Matsumoto, T. [1986] "The double scroll family," *IEEE Trans. Circuits Syst.* **33**, 1072–1118.
- Elwakil, A. S. & Kennedy, M. P. [2000] "Improved implementation of Chua's chaotic oscillator using current feedback op amp," *IEEE Trans. Circuits Syst.-I* **47**, 76–79.
- Elwakil, A. S., Özoğuz, S. & Kennedy, M. P. [2003] "A four-wing butterfly attractor from a fully autonomous system," *Int. J. Bifurcation and Chaos* **13**, 3093–3098.
- Han, F., Lü, J., Yu, X., Chen, G. & Feng, Y. [2005] "Generating multi-scroll chaotic attractors via a linear second-order hysteresis system," *Dyn. Contin. Discr. Impul. Syst. Ser. B* **12**, 95–110.
- Kennedy, M. P. [1993] "Three steps to chaos. II. A Chua's circuit primer," *IEEE Trans. Circuits Syst.-I* **40**, 657–674.
- Li, Y., Tang, W. K. S. & Chen, G. [2005] "Generating hyperchaos via state feedback control," *Int. J. Bifurcation and Chaos* **15**, 3367–3375.
- Lü, J. & Chen, G. [2002] "A new chaotic attractor coined," *Int. J. Bifurcation and Chaos* **12**, 659–661.
- Lü, J., Chen, G., Cheng, D. Z. & Celikovskiy, S. [2002] "Bridge the gap between the Lorenz system and the Chen system," *Int. J. Bifurcation and Chaos* **12**, 2917–2926.
- Lü, J., Yu, X. & Chen, G. [2003] "Generating chaotic attractors with multiple merged basins of attraction: A switching piecewise-linear control approach," *IEEE Trans. Circuits Syst.-I* **50**, 198–207.
- Lü, J., Chen, G. & Cheng, D. Z. [2004a] "A new chaotic system and beyond: The general Lorenz-like system," *Int. J. Bifurcation and Chaos* **14**, 1507–1537.
- Lü, J., Chen, G., Yu, X. & Leung, H. [2004b] "Design and analysis of multi-scroll chaotic attractors from saturated function series," *IEEE Trans. Circuits Syst.-I* **51**, 2476–2490.
- Lü, J., Han, F., Yu, X. & Chen, G. [2004c] "Generating 3-D multi-scroll chaotic attractors: A hysteresis series switching method," *Automatica* **40**, 1677–1687.
- Lü, J. & Chen, G. [2006] "Multi-scroll chaos generation: Theories, methods and applications," *Int. J. Bifurcation and Chaos* **16**, 775–858.
- Lü, J., Yu, S. M., Leung, H. & Chen, G. [2006] "Experimental verification of multi-directional multi-scroll chaotic attractors," *IEEE Trans. Circuits Syst.-I* **53**, 149–165.
- Matsumoto, T., Chua, L. O. & Kobayashi, K. [1986] "Hyperchaos: Laboratory experiment and numerical confirmation," *IEEE Trans. Circuits Syst.-I* **33**, 1143–1147.
- Suykens, J. A. K. & Vandewalle, J. [1993] "Generation of n -double scrolls ($n = 1, 2, 3, 4, \dots$)," *IEEE Trans. Circuits Syst.-I* **40**, 861–867.
- Tang, K. S. & Man, K. F. [1998] "An alternative Chua's circuit implementation," *Proc. 1998 IEEE Symp. Industrial Electronics*, Pretoria, South Africa, Jul. 7–10, pp. 441–444.
- Tang, K. S., Zhong, G. Q., Chen, G. & Man, K. F. [2001] "Generation of n -scroll attractors via sine function," *IEEE Trans. Circuits Syst.-I* **48**, 1369–1372.
- Yalcin, M. E., Suykens, J. A. K. & Vandewalle, J. [2000] "Experimental confirmation of 3- and 5-scroll attractors from a generalized Chua's circuit," *IEEE Trans. Circuits Syst.-I* **47**, 425–429.
- Yalcin, M. E., Suykens, J. A. K., Vandewalle, J. & Ozoguz, S. [2002] "Families of scroll grid attractors," *Int. J. Bifurcation and Chaos* **12**, 23–41.
- Yin, Y. Z. [1997] "Experimental demonstration of chaotic synchronization in the modified Chua's oscillators," *Int. J. Bifurcation and Chaos* **7**, 1401–1410.

- Yu, S. M., Lin, Q. H. & Qiu, S. S. [2004a] "A family of multiple-folded torus chaotic attractors," *Acta Phys. Sin.* **53**, 2084–2088.
- Yu, S. M., Ma, Z. G., Qiu, S. S., Peng, S. G. & Lin, Q. H. [2004b] "Generation and synchronization of n -scroll chaotic and hyperchaotic attractors in fourth-order systems," *Chin. Phys.* **13**, 317–328.
- Yu, S. M., Lü, J., Leung, H. & Chen, G. [2005] "Design and circuit implementation of n -scroll chaotic attractor from a general jerk system," *IEEE Trans. Circuits Syst.-I* **52**, 1459–1476.
- Zhong, G. Q. [1994] "Implementation of Chua's circuit with a cubic nonlinearity," *IEEE Trans. Circuits Syst.-I* **41**, 934–941.
- Zhong, G. Q., Man, K. F. & Chen, G. [2002] "A systematic approach to generating n -scroll attractors," *Int. J. Bifurcation and Chaos* **12**, 2907–2915.
- Zhong, G. Q. & Tang, W. K. S. [2002] "Circuitry implementation and synchronization of Chen's attractor," *Int. J. Bifurcation and Chaos* **12**, 1423–1427.